



HAL
open science

Study of delamination of fibre harness satin weave composites molded by hot pressing. The example of high strength carbon fiber and PEEK matrix

Georges Kamgaing Somoh, Pongsak Nimdum, Jacques Renard

► **To cite this version:**

Georges Kamgaing Somoh, Pongsak Nimdum, Jacques Renard. Study of delamination of fibre harness satin weave composites molded by hot pressing. The example of high strength carbon fiber and PEEK matrix. ECCM 15 - 15th European Conference on Composite Materials, Jun 2012, Venice, Italy. 8 p. hal-01109506

HAL Id: hal-01109506

<https://minesparis-psl.hal.science/hal-01109506>

Submitted on 26 Jan 2015

HAL is a multi-disciplinary open access archive for the deposit and dissemination of scientific research documents, whether they are published or not. The documents may come from teaching and research institutions in France or abroad, or from public or private research centers.

L'archive ouverte pluridisciplinaire **HAL**, est destinée au dépôt et à la diffusion de documents scientifiques de niveau recherche, publiés ou non, émanant des établissements d'enseignement et de recherche français ou étrangers, des laboratoires publics ou privés.

Study of delamination of five harness satin weave composites molded by hot pressing. The example of high strength carbon fiber and PEEK matrix.

G. Kamgaing^{*}, P. Nimdum, J. Renard

Centre des Matériaux P. M. Fourt, Mines-Paris Tech, CNRS UMR 7633, BP 87, F-91003 Evry cedex
**georges.kamgaing@mines-paristech.fr*

Keywords: five harness satin weave, delamination criterion identification, acoustic emission, mesoscopic scale modeling.

Abstract

The purpose of this study is to identify a delamination criterion and find a way to apply it directly on industrial parts. Criterion parameters are identified using edge delamination tests and observations. The experimental setup is equipped with a camera and a data recording system of acoustic emissions to detect the onset of the delamination and its propagation. The identified criterion is then validated on a laboratory sample and applied to a real part modeled at mesoscopic scale (ply scale). These results give interesting prospects for a less conservative design. In fact, since the appearance of a macroscopic delamination coincides with the start of a fall of mechanical properties, a good prediction of this phenomenon would significantly reduce safety factors applied to aerospace components today.

1. Introduction

The prediction of delamination is a complex problem that has interested many researchers. Early work on this subject started in 80s with Herakovich [1] which showed that this defect occurs preferentially at the $+\theta$ / $-\theta$ interfaces of laminates subjected to uniaxial tension. Then Kim and Soni [2] were proposed the formulation of a quadratic and non-local delamination criterion. This criterion has then been modified by several authors [3]. Brewer and Lagace [3] demonstrated the sensitivity of the delamination onset and propagation with increasing laminate thickness. Based on the work of Brewer and co-workers [4] have proposed a method based on edge delamination test (EDT) to identify the criteria parameters. More recently, Nimdum [5] and Bassery [6] modified the Kim's criterion by taking into account the influence of friction between laminate plies on delamination strength. Also in the 90s, another approach for the prediction of delamination based on the fracture mechanics has been developed a lot in composites. This approach considers the delamination as a crack and measures the energy release rate during its propagation. Bathias [7] has reviewed full of these methods. In comparison with Kim's approach, it fairly requires complex tests, so called DCB tests, to result in more expensive to perform.

Despite these numerous studies, delamination remains a crucial question. In fact, the majority of the conventional design criteria of composite components are based on the final failure of the laminates. This approach necessarily requires a high safety factor which finally is an ignorance factor. As well-known, before the final fracture, several damage mechanisms occur in the material. It would be judicious to act earlier, for example at the delamination onset which is the prior phase to the fracture. This approach has been implemented successfully by

Nimduim [5] and Bassery [6]. However, these approaches were validated only on laboratory test specimens. In this reason, the main aims of this investigate are, firstly, to identify the delamination criterion for the five harness carbon/PEEK satin weave, and then to propose a generic method which can be applied for industrial structures..

2. Materials

The material of this study is carried out on high strength carbon HTA/PEEK composite material. The weave is a five harness satin balanced in warp and weft directions and the thermoplastic PEEK matrix is Evonik's type. Laminates are manufactured by Carbone Forge Company using a hot pressing process of impregnated fabrics, so-called prepregs. Prepregs are 3K type with an area density of 477g/m² and a fiber weight fraction of 0.6. After molding, the laminates have an average ply thickness of 0.3mm and 0.52 as fiber volume fraction.

To evaluate the orthotropic stiffness matrix of a single ply, necessary for finite element calculations, only six elastic constants E_1 , E_3 , G_{12} , G_{13} , ν_{12} and ν_{13} (where the subscripts 1, 2 and 3 indicate respectively warp, weft and thickness directions) are required since warp and weft directions are equivalent. E_1 , G_{12} , G_{13} and ν_{12} are experimentally obtained by tensile, bending and intralaminar shear tests on 2mm thick laminates. To determine the Young Modulus E_3 in thickness direction, a compression test on 4 mm thick cylindrical rod was carried out with the assumption that the Young modulus in tensile and compression are equivalent. Due to the high difficulty to measure the ν_{13} by experimental test, we choose this value to be 0.4 which commonly used for this type of material. Finally, the single ply properties are summarized in table 1.

E_1 [MPa]	E_3 [MPa]	G_{12} [MPa]	G_{13} [MPa]	ν_{12}	ν_{13}
57600	8350	4500	1510	0,05	0,40

Table 1. Summary of the elastic properties of the elementary ply

3. Criterion and Identification.

3.1. Criterion.

In the same manner as cracks growth, delamination occurs in 3 modes including one opening mode (mode 1) and two shear modes (modes 2 and 3). To predict its initiation, we used an approach based on the stress tensor component. In comparison with the fracture mechanics approach, this one is easier to use by designers since the stress field are directly available over the finite element calculations. Kim and Soni in 1984 [2] were, firstly, to propose a formulation of the criterion given in equation (1):

$$\left(\frac{\bar{\sigma}_{xz}}{\sigma_{xz}^D}\right)^2 + \left(\frac{\bar{\sigma}_{yz}}{\sigma_{yz}^D}\right)^2 + \bar{\sigma}_{zz} \left(\frac{1}{\sigma_{zz}^{DT}} - \frac{1}{\sigma_{zz}^{DC}}\right) + \left(\frac{\bar{\sigma}_{zz}^2}{\sigma_{zz}^{DT} \sigma_{zz}^{DC}}\right) = 1 \quad (1)$$

Where σ_{xz}^D and σ_{yz}^D represent the delamination strenght in shear modes (modes 2 and 3),

σ_{zz}^{DT} the delamination strenght in opening mode (mode 1 in tension),

σ_{zz}^{DC} the delamination strenght in compression mode (mode 1 in compression),

$\bar{\sigma}_{ij} = \frac{1}{y_0} \int_0^{y_0} \sigma_{ij} dy$ the average stress of σ_{ij} at y_0 distance from the free edge.

As can be seen, this criterion is an interactive one as Tsai criteria but introduced the concept of average stress over a critical distance, making it a non-local criterion. Beside, it also takes in account the compression effect to tension in open mode. This criterion will be simplified by

omitting the compression term in mode I. By taking into account the Coulomb effects, the delamination strength in shear mode is affected by normal compression force which generates frictions between layers. Then, we are able to simplify this criterion given by equation (2) where k_1 and k_2 are friction coefficients in shear modes 2 and 3 respectively.

$$\left(\frac{\bar{\sigma}_{xz}}{\sigma_{xz}^D}\right)^2 + \left(\frac{\bar{\sigma}_{yz}}{\sigma_{yz}^D}\right)^2 + \frac{\bar{\sigma}_{zz}}{\sigma_{zz}^{DT}} = 1 \text{ if } \bar{\sigma}_{zz} > 0 \text{ or } \left(\frac{\bar{\sigma}_{xz}}{\sigma_{xz}^D - k_1 \bar{\sigma}_{zz}}\right)^2 + \left(\frac{\bar{\sigma}_{yz}}{\sigma_{yz}^D - k_2 \bar{\sigma}_{zz}}\right)^2 + \frac{\bar{\sigma}_{zz}}{\sigma_{zz}^{DC}} = 1 \text{ if } \bar{\sigma}_{zz} < 0 \quad (2)$$

By equation (2), we can make one more assumption to further simplify. First we assume that all modes of delamination growth have the same critical distance y_0 . Then, we assume that the two shear modes are equivalent, i.e. $\sigma_{xz}^D = \sigma_{yz}^D$ and $k_1 = k_2 = k$. Finally, Only 4 parameters will be identified, namely σ_{zz}^{DT} , σ_{xz}^D , y_0 and k .

3.2. Parameters identification

3.2.1. σ_{zz}^{DT} parameter.

In order to measure this parameter, we need to apply a load at the interface in opening mode. To do that, the Arcan-Mines test as describe in ref. [6] was realized. However, this test is extremely difficult to implement. Then, we propose a new system which is more simple as described in figure 1. Cylindrical samples of 4 mm in thickness and 22 mm in diameter are joined carefully on an aluminum support with special glue for thermoplastic polymers. In order to endure the failure at interface layer, not only a notched specimen with 2mm in thickness and 5mm in width was cut around the rod but also a special system for engaging the lips of the notched sample is added. Then, this specimen was performed by Instron machine in thickness direction under tensile test.

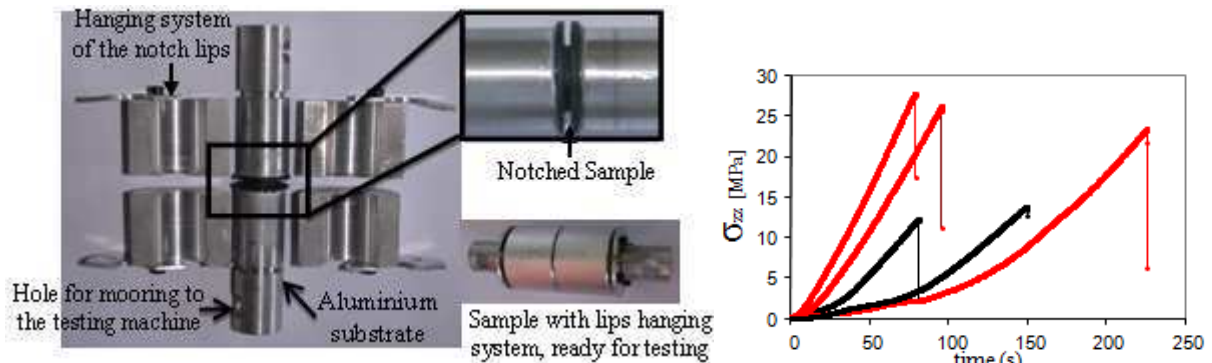


Figure 1. Delamination test specimen in opening mode (right) and results (left)

Figure 1 shows the important role of the hanging system (red curves) resulted in high failure strength in comparison with not using this system. Finally, these results allow us to identify the delamination strength in open mode to 26 MPa (average value).

3.2.2. y_0 , σ_{yz}^D and k parameters

To assess these parameters, we used the method proposed by Lecuyer and co-workers which have been widely used in numerous studies [4,5,8]. First, edge delamination tests (EDTs) were performed on specific laminates which has a tendency to present delamination in shear mode. The delamination onset stress was recorded. Then, by using numerical results which simulate at similar macroscopic stress level in experimental result, the delamination strength was determined.

3.2.2.1. Experimental measurement of the delamination load.

As explained in above, we selected $(0^\circ, \pm 20^\circ)_n$ s and $(0^\circ, \pm 30^\circ)_n$ s laminates with $n = 1$ and 2, which are known to be very sensitive to shear delamination at $+\theta/-\theta$ interfaces. The tensile specimens are prepared according to European standard EN2561 and the free edge was polished in order to easier observe by a camera during testing. The test samples are also equipped with acoustic emission system for monitoring various damage which occur during load applied. A crosshead travel rates of 0.25mm/min was chosen in order to prevent saturation of the acoustic recorder system. More information about the acoustic emission test is available in [9].

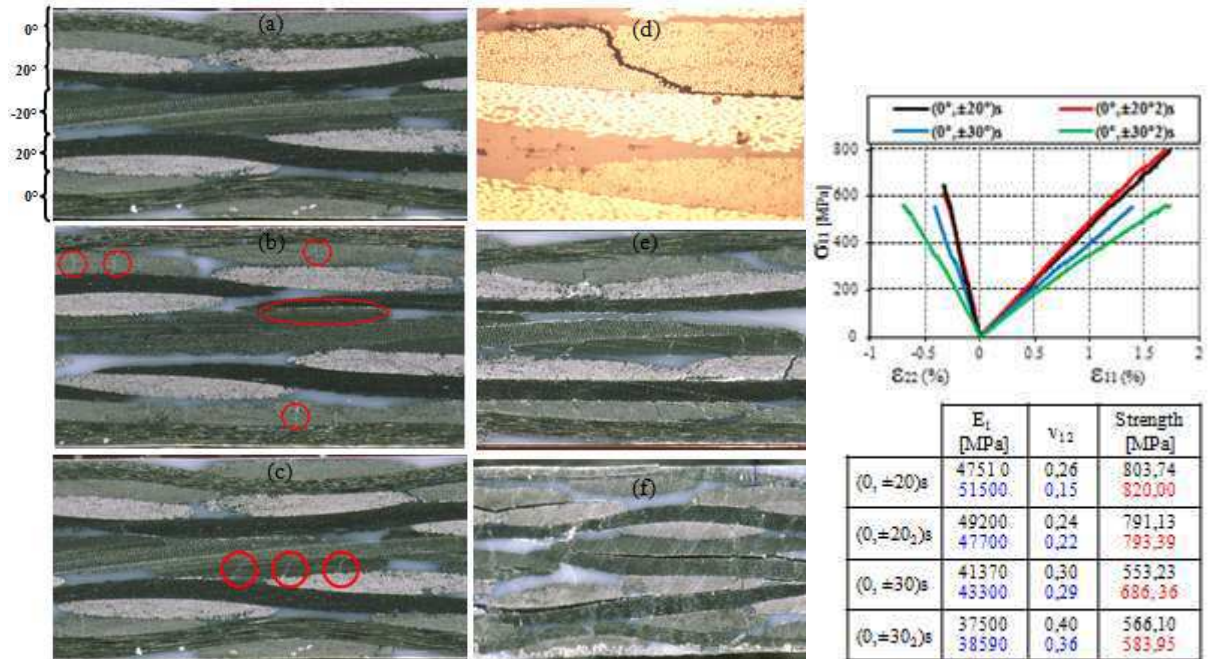


Figure 2. In situ observation of the $(0^\circ, \pm 20^\circ)_s$ laminate and Stress-strain curves for 2mm/min load rate. In black in the table, values for 2mm/min; in red values for 0.25 mm/min; in blue values from laminate theory

Figure 2 shows the mechanical properties of laminates at different load rate. These results which are close to those obtained by applying laminate theory validate single ply properties (see in the table 1) that we used in finite element simulation.

Figure 2 also shows camera in situ observations of the $(0^\circ, \pm 20^\circ)_s$ laminate and illustrates the material degradation process until failure. The picture Figure 2(a) represents the material prior to apply load. We can notice that interfaces between adjacent layers are not regular plans as in unidirectional laminates. Up to about 40% of failure stress, the material microstructure remains unchanged until 40% (picture (b)) first crack growth occurs on weft (transverse) yarns of 0° layers. This is quite logical fact since these layers carry most of the load lead to be first affect. Beside, we also found the discrete white marks occurring at the interfaces that we assume to be fibre/matrix debonding (micro-delaminations). When the loading continues increase, these white marks become more and more numerous and seem to coalesce to form nearly continuous lines. Up to around the 60% of failure stress (Figure2(c)), the first crack occurs on yarns of 20° layer. This phenomenon represents to the limitation of load transfer to the 0° layers. When the loading continues increase up to about 95% of failure stress (Figure 2(e)), 0° and 20° layers show several open transverse cracks in their weft yarns. Figure 2(f) shows the specimen just before failure in an area near the breaking zone. We found that the significant delamination appear in this zone to confirm the important role of the delamination. Figure 2(d) show the optical microscopic observation after the specimen failure to confirm the

white marks which were observed by camera. In the similar procedure as $(0^\circ, \pm 20^\circ)_s$ stacking sequence, five layers of $(0^\circ, \pm 30^\circ)$ laminate were done.

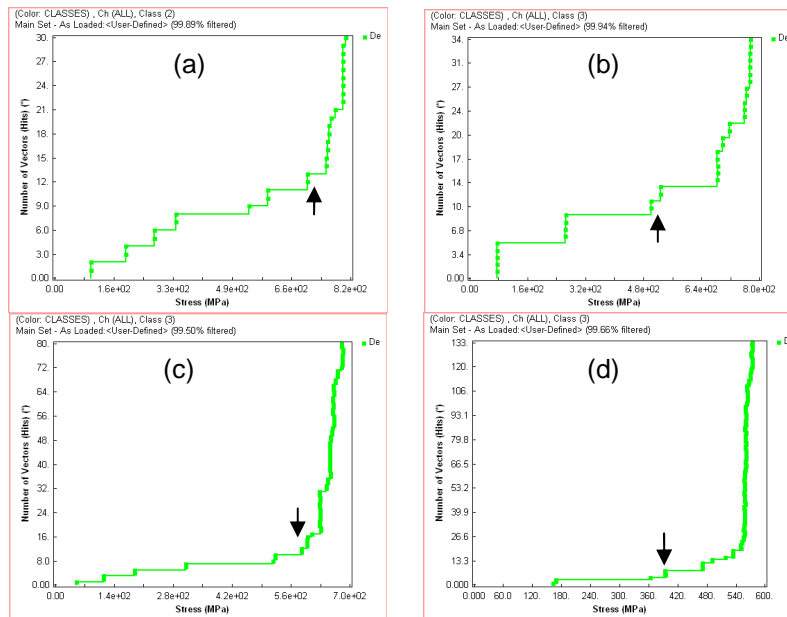


Figure 3. Spectra of number of high energy and long duration events versus stress applied for. (a) $(0^\circ, \pm 20^\circ)_s$; (b) $(0^\circ, \pm 20^\circ)_2s$; (c) $(0^\circ, \pm 30^\circ)_s$; (d) $(0^\circ, \pm 30^\circ)_2s$. Arrows indicate the beginning of propagation.

According to these results, we can deduce that propagation of the delamination of five layers laminates occurs around 90% of their axial strength (values in red line in figure 4). In fact, we think that any propagation can't occur before transverse cracks saturation in the material and the appearance of several open cracks in 20° or 30° layers which finally act to delay the propagation of delamination to correspond to the summary of Bathias's work [7]. For 8 layers laminates $(0^\circ, \pm 20^\circ)_2s$ and $(0^\circ, \pm 30^\circ)_2s$, this saturation stage occurs very early to around 60% of their longitudinal tensile strength which confirms the thickness effects as shown in Brewer and Lagace [3]. This summary should be verified by acoustic emission monitored.

By using data recording of acoustic emissions (number, duration, amplitude, frequency, energy and cumulative energy of events), the duration and energy are good parameters to represent the damage developed during the tensile loading. We found that delamination produce the long duration and high energy signal since it involves high energy release to create the separations of large surfaces. Figure 3 shows the cumulative number events of high energy signals as function of applied stress. The step increasing level in first stage represents an isolated delamination which occurs at intersection of warp yarn. When the cracks density will be enough in the material, these isolated delaminations will coalesce and the macroscopic propagation will start. This phenomenon will correspond to sudden increase in event numbers. Finally, we can determine the delamination onset stress around 740 MPa, 490 MPa, 620 MPa and 360 MPa for $(0^\circ, \pm 20^\circ)_s$, $(0^\circ, \pm 30^\circ)_s$, $(0^\circ, \pm 20^\circ)_2s$ and $(0^\circ, \pm 30^\circ)_2s$ laminates, respectively. These values are good agreement with previously results by camera observations.

3.2.2.2. Simulations of tensile tests and parameter's identification.

This section show the simulation results of the tensile tests performed on the laminates at delamination onset stress (previously identified). Figure 4 shows the mesh by using 8 Gauss points of linear cubic elements (C3D8). On a small area close to the free edge, the mesh refinement is done with element's size equal to one sixth of the thickness. Then two types of nodes lines are created: one at free edge in the thickness direction (z direction). The second one at $+\theta/-\theta$ interface in y direction along which will be applied the criterion given by

equation (2). At each node of the lines are stored coordinates and local stresses. Another script retrieves these data and automatically computes the average stress along the nodes lines. Finite element simulations are performed with commercial software Zebulon developed at “Centre Des Matériaux de l’écôle des mines Paris”. Results are shown in Figure 5.

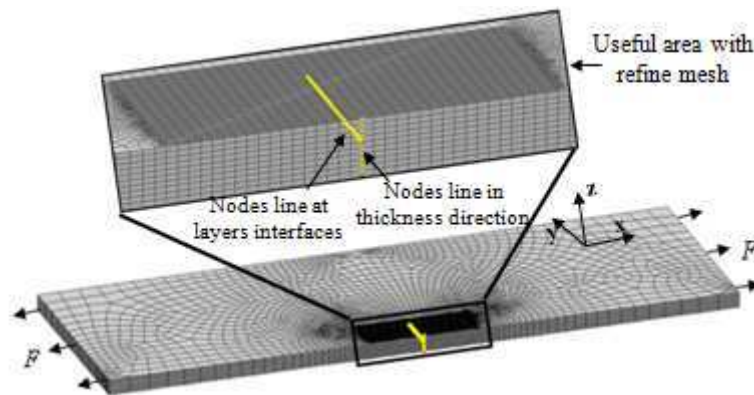


Figure 4. 3D Mesh of tests specimens for finite element calculations

The first picture (a) shows the friction case which exist the normal compression stresses at all interfaces. According to Lecuyer’s work [4] proposed that the critical distance and the shear mode delamination strength are materials properties, then all curves should intersect at the same point where this coordinates should correspond to these two parameters. However, as can be seen the second picture (b), all curves intersect at the same abscissa which is about 0.3mm but at two different average stresses. Curves of (0°,±20°)s laminates intersect at 56 MPa and those of (0°,±30°)s laminates intersect at 42 MPa, i.e. 49 MPa (average value). This difference in stress level can be explained by the fact that this second image does not include the friction effects which are particularly high in (0°,±30°)s laminates as shown in the first image.

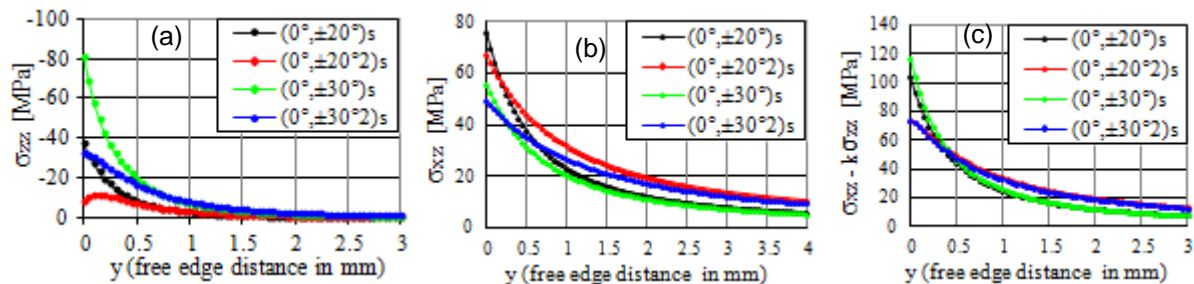


Figure 5. Average stresses in function of the distance to the specimen free edge: (a) normal stress without friction effects ($k=0$), (b) shear stress without friction effects ($k=0$); (c) shear stress with friction effects ($k=0.75$)

In order to take into account friction effects, we select the value of k to 0.75 according to the Bassery’s work [6] which investigate on a five harness carbon/PPS satin weave. If we plot the average shear stress adding to the friction effects as a function of free edge distance, we obtain the last picture (c). We see that all curves now intersect at the same point which coordinates are around 0.3mm and 55 MPa. Table 3 summarizes all identified parameters.

y_0 [μm]	σ_{zz}^D [MPa]	$\sigma_{xz}^D = \sigma_{yz}^D$ [MPa]	k
300(~ply thickness)	25,78	49/55	0,75

Table 1. Summary of criterion parameters; in red value with friction effects.

4. Criterion validation

4.1. Application to a laboratory test specimen.

To validate our criterion, we choose, firstly, to apply it on a laboratory tensile specimen. The material is an 8 layers (+20°, +10°, -50°)₂s laminate. The calculation procedures are the similar procedure described previously.

Simulation results in figure 6 show that the +20°/-10° interface is the most susceptible to delamination onset. According to curves of the criterion value as a function of applied stress, delamination occurs firstly at this interface around 400 MPa. Then, in next step, this numerical result will be verified with experimental result (waiting to receive specimen from my industrial partner).

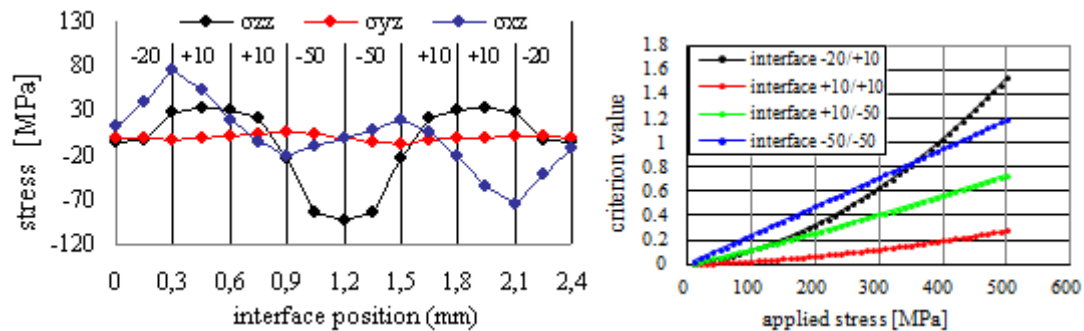


Figure 6: out of plane stresses at free edge in thickness direction and criterion value evolution with applied tensile stress. Vertical grids on the first picture indicate interface positions.

4.2. Application to a structure.

The second application concerns a simple structure specimen, so-called omega, which mesh is shown in figure 9. It is 300mm long and 30mm wide and consists of eight layers of a quasi-isotropic (0°, +90°, ±45°)_s laminate. The numerical simulation concerns at meso scale (ply scale) which local coordinate are defined at each element of each layer as shown in figure 7. To apply our criterion, the mesh refinement is requested. However, it is clear that we cannot refine the whole of specimen since too heavy computational time for a finite elements calculation. To resolve that, five parts of specimen were defined as shown in figure 7: (a), (b), (c), (d) and (e). By numerical simulation, we found that the zone (d) represent as the critical area under load applied. In this reason, the refinement mesh is required (a size of elements equal to one sixth of the thickness). Then, this area (d) is joined to the rest of the specimen by using tie contact conditions which does not interfere significantly the stress field. As previous simulations, node lines are created at the interfaces between plies and the same criterion computing procedure is applied.

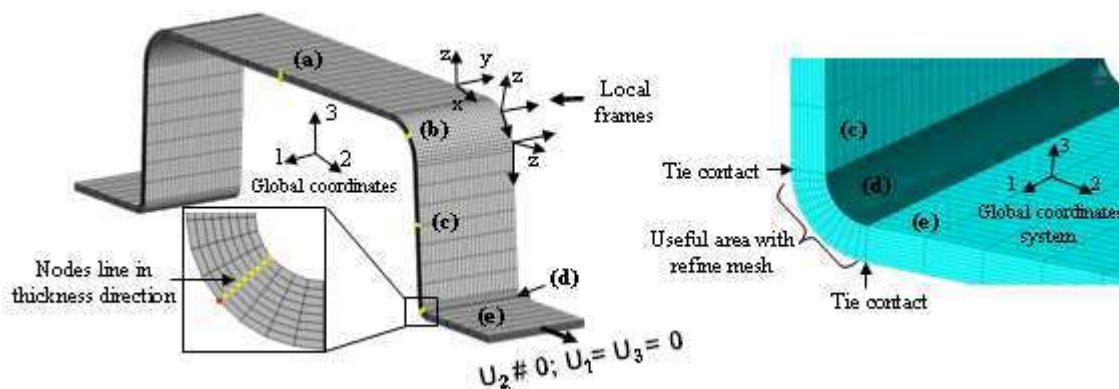


Figure 7: Mesh of the omega part

The simulation results as shown in figure 8 illustrate that the open mode of delamination is the most important. Also, the 0°/90° interface is the most sensitive. The curve of criterion value as a function of displacement lead us to predict the delamination at 0°/+90° interface for an applied displacement U_2 equal to 4.25mm. In the same manner in above, these results will be experimentally verified as soon I receive the molding part and this paper will be up date.

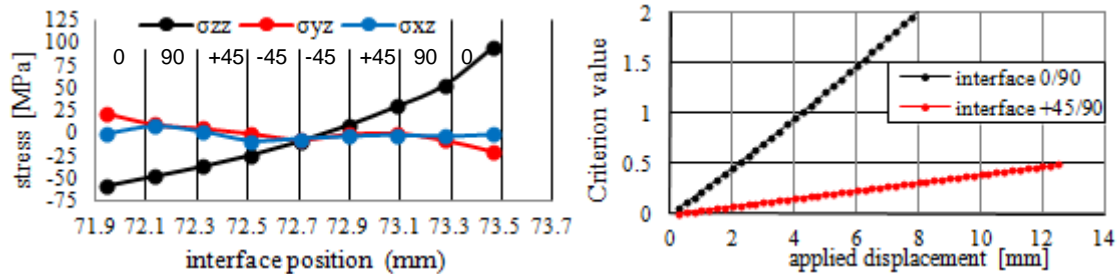


Figure 8. Out of plane stresses at free edge in thickness direction (left) and criterion evolution with applied displacement (right). Vertical grids on the first picture indicate interface positions

5. Conclusion

In this study, we have successfully identified a delamination criterion and proposed an approach for a direct application to industrial parts. The first results are encouraging and open up prospects for a design closer to the damage mechanisms occurring in the material, which could significantly reduce the safety factors in particularly high for aerospace applications (six time of standard deviation). However, in order to obtain high reliability in design, several parameters will be improved. First, the detect system should be improved in order to be more precise on delamination onset and its propagation. It remains difficult to use AE system in composite woven since the delamination occurs very early. Otherwise, the mesh generation software methods would be developed result in the simplification for numerical simulation in order to apply this criterion in structure specimen.

AKNOWLEDGEMENTS

We gratefully acknowledge all partners in the project CRISTAL (Carbone foRge Improved procesS forTechnological Advance Level) for support to ARMINES Centre des Matériaux.

REFERENCES

- [1] Herakovich C. T. On the relationship between engineering properties and delamination of composite materials. *J. Composite materials*, vol. 15, pp. 336-348, 1981.
- [2] Kim R. Y., Soni S. R. Experimental and analytical studies on the onset of delamination in laminated composites. Criterion for initiation of delamination. *J. Composite materials*, vol. 18, pp. 70-80, 1984.
- [3] Brewer J. C., Lagace P. A. Quadratic stress criterion for initiation of delamination. *J. Composite materials*, vol. 22, pp. 1141-55, 1988.
- [4] Lecuyer F., Engrand D. *A methodology for the identification of a criterion for delamination initiation*. "Proceeding of 8th National Days of Composites (JNC 8)" Paris, France, 1992.
- [5] Pongsak N. Comportement de composites tissés épais soumis à des sollicitations quasi statiques. *Revue des composite et des matériaux avancés*, vol. 13, pp. 41-80, 2010
- [6] Bassery J., Renard J. Etude du délaminage en fatigue des composites tissés carbone/PPS. *Revue des Composites et des Matériaux Avancés*, vol. 10, pp. 345 – 380, 2011.
- [7] Bathias Claude. "Une revue des méthodes de caractérisation du délaminage des matériaux composites." *Annales des Composites*, vol. 1, pp. 5-25, 1995.
- [8] Lorriot Th. Onset of free-edge delamination in composite laminates under tensile loading. *Composites part B*, vol. 34, pp. 459-471, 2003.
- [9] Pongsak N., Renard J. *Use of acoustic emission to discriminate damage modes in carbon fibre reinforced epoxy laminate during tensile and buckling loading*. "Proceeding of 15th European Conference on Composite Materials", Venice, Italy, 24 -28 June 2012.